

Laser-induced charge-transfer collisions of calcium ions with strontium atoms

M. D. Wright, D. M. O'Brien, J. F. Young, and S. E. Harris

Edward L. Ginzton Laboratory, Stanford University, Stanford, California 94305

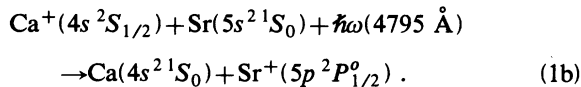
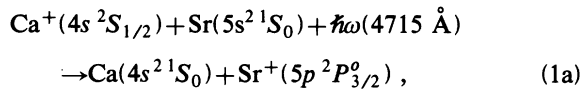
(Received 23 April 1981)

Experimental studies of two laser-induced charge-transfer reactions in Ca and Sr are presented. In both reactions, a Ca ion collides with an Sr neutral in the presence of a laser field to produce a Ca neutral and an excited Sr ion. The two reactions differ in the final level of the Sr⁺ species. The collision cross sections associated with these reactions are studied as functions of applied laser frequency and power density. The largest cross section induced is equal to 10⁻¹⁶ cm², obtained at a power density of 2 × 10⁹ W/cm². Differences in experimental results associated with the two reactions are explained qualitatively by an examination of the potential curves of the CaSr⁺ quasimolecule.

I. INTRODUCTION

Laser-induced collision processes constitute a technique for energy transfer in atomic systems and as such may have application to the development of high-energy visible and ultraviolet lasers. For example, an electrical discharge might be used to create a large metastable population in one species and the stored energy could then be rapidly transferred by laser-induced collisions to a lasing level in a second species. A laser-induced charge-transfer collision¹⁻⁵ is a particularly interesting process in that it exploits a high-capacity storage species, ground-state ions. Ions are easily created and have long lifetimes.

In this publication we present an experimental study of two laser-induced charge-transfer collision processes:



An energy-level diagram pertinent to both processes is shown in Fig. 1. Without the laser photon the processes of Eq. (1) are endothermic and have a vanishingly small collision cross section. The laser photon supplies necessary energy and may be thought of as raising one of the two Sr valence electrons to a virtual level of Sr(5s 5p¹P^o) character. The Sr atom in a virtual level then collides with a ground-state Ca ion which captures the remaining Sr valence electron, leaving a Ca ground-state neutral and an excited Sr ion.

The laser-induced charge-transfer collisions given by Eqs. (1a) and (1b) appear quite similar, the final levels of the target species differing only in *J* value. However, there are significant differences in the character of the two reactions. In a laser-induced charge-transfer collision, the collision cross section maximizes at a wavelength which is detuned from the wavelength of the photon which exactly satis-

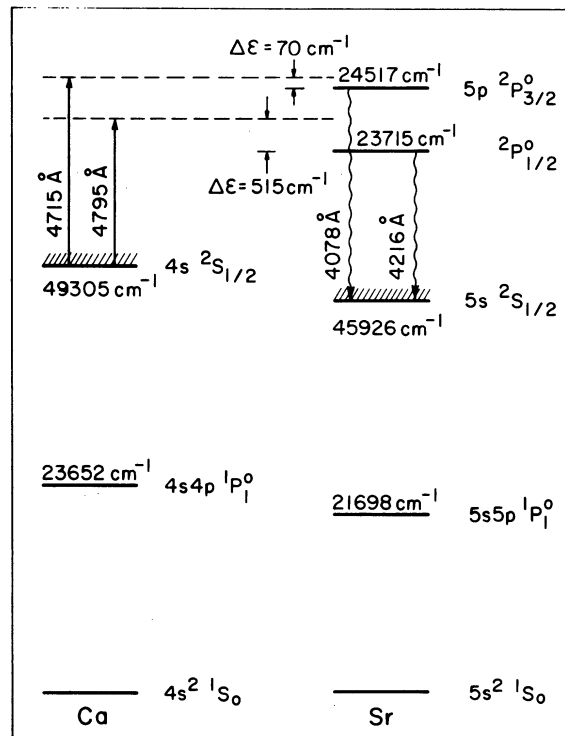


FIG. 1. Energy level diagram for laser-induced charge-transfer reactions (1a) and (1b).

fies the energy defect between the initial and final states of the collision system when the colliding species are infinitely separated ($\lambda_{R=\infty}$). As indicated in Fig. 1, the cross section associated with reaction (1a) maximizes when the photon is 70 cm^{-1} more energetic than $\lambda_{R=\infty}$, while the cross section associated with reaction (1b) maximizes when the photon is 515 cm^{-1} more energetic than $\lambda_{R=\infty}$. Also, the values and line shapes of the cross sections for reactions (1a) and (1b) are considerably different. These differences are a result of the quasimolecular potentials associated with the different target levels.

II. APPARATUS

In order to observe the charge-transfer processes described by Eqs. (1a) and (1b), two lasers are used: one to produce Ca^+ population for energy storage, and the second to affect energy transfer to the excited Sr^+ level. A schematic of the optical system employed to observe reaction (1a) is shown in Fig. 2. An actively mode-locked and Q -switched Nd:YAG (yttrium aluminum garnet) oscillator generates $\sim 2 \text{ mJ}$ of $1.06\text{-}\mu\text{m}$ radiation in a train of pulses. Each pulse is 100 ps in duration and there are about 10 pulses in the train. The pulse train is amplified by a series of Nd:YAG amplifiers having a final aperture of 0.95 cm and typically supplying a total of 300 mJ . Two KD*P (potassium dideuterium phosphate) crystals are used to generate $3547\text{-}\text{\AA}$ radiation by successive second harmonic generation and mixing. The $\sim 90 \text{ mJ}$ of $3547\text{-}\text{\AA}$ radiation is separated by a prism, split, and used to pump two dye lasers. Each dye laser is synchronously pumped,⁶ prism tuned, and cavity dumped to produce a single 40 ps pulse of tunable visible radiation with an energy of from 0.1 to 0.5 mJ and a linewidth of $\sim 10 \text{ cm}^{-1}$. The two dye laser

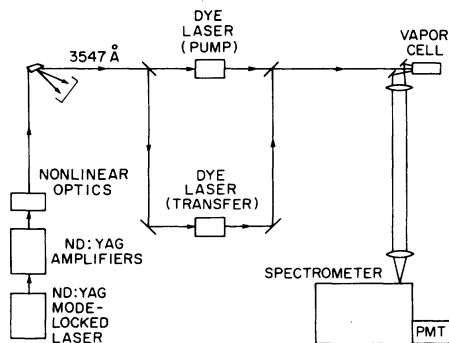


FIG. 2. Schematic of optical system used to observe reaction (1a).

pulses are spatially combined with a dichroic mirror and focused to an area of 10^{-3} cm^2 inside the metal vapor cell. Thus, power densities of several GW/cm^2 are available. The metal vapor cell is heated to $\sim 850^\circ\text{C}$ and produces ground-state densities of about 10^{16} cm^{-3} of both Sr and Ca; 15 torr of argon buffer gas is used to protect the cell windows.

The wavelength of the pump dye laser is tuned to 5361 \AA , which corresponds to the $\text{Ca}(4s^2^1S_0)\text{-Ca}(4s4d^1D_2)$ two-photon transition. Ca ions are produced by resonantly enhanced three-photon ionization. The pulse from the transfer laser arrives in the cell 5 ns after the pump laser pulse to eliminate possible two-photon effects. Back-directed fluorescence from the target level population created by the laser-induced charge-transfer process is collected by a mirror with a hole in it and focused into a 1-m spectrometer having a resolution of 2.5 \AA and an RCA 31034 photomultiplier at its exit slit.

In order to observe the laser-induced charge-transfer process denoted by Eq. (1b), more energy in the transfer laser pulse is required than that which can be delivered by the transfer laser system described above. Therefore, a Quanta-Ray PDL dye laser is used as the transfer laser. A schematic is shown in Fig. 3. The Quanta-Ray dye laser produces about 10 mJ in the desired wavelength region with a spectral linewidth of about 0.5 cm^{-1} and a pulse duration of 5 ns . In this configuration the transfer laser pulse follows the pump laser pulse by about 30 ns . The longer delay between pump and transfer laser pulses is necessary because of the greater jitter in pulse timing using two independent lasers.

In both charge-transfer experiments the transfer laser wavelength is scanned and the intensity of fluorescence from the target level population is

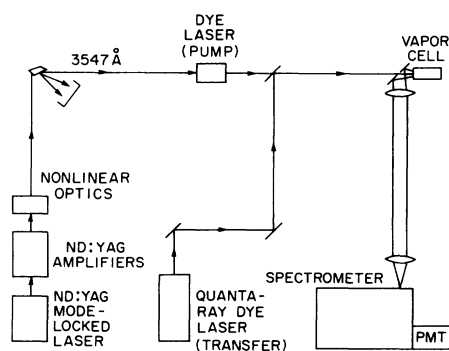


FIG. 3. Schematic of optical system used to observe reaction (1b).

recorded both as a function of the transfer laser wavelength and as a function of time. Time resolution is accomplished by processing the signal from the photomultiplier with four electronic integrators which are gated on during consecutive 10-ns time intervals. The outputs of the integrators are input to a Cromemco Z-2D minicomputer which stores the information on a disk for later data smoothing.

Determination of collision cross sections associated with reactions (1a) and (1b) requires the measurement of the initial Ca^+ population density as well as the measurement of the excited Sr^+ densities. Excited Sr^+ densities are determined from the fluorescent signals which are produced during the experimental procedures described above. The Ca^+ population density is determined by measuring the absorption of a probe beam at 3934 Å corresponding to the $\text{Ca}^+(4s^2S_{1/2})-\text{Ca}^+(4p^2P_{3/2}^o)$ transition. The apparatus used to make this measurement is the same as that shown in Fig. 3, with the modification that the spectrometer is moved directly behind the cell such that the probe laser beam passes through the entrance slit of the spectrometer after emerging from the cell.

III. RESULTS

Scans associated with reaction (1a) are presented in Fig. 4. In this figure, fluorescence at 4078 Å is plotted as a function of transfer laser wavelength for each of the sequential 10-ns observation time intervals. The laser-induced charge-transfer signal peaks at 4715 Å. The line shape associated with this process is characterized by a slight tail on the blue side of the peak and a width of $\sim 50 \text{ cm}^{-1}$ full width at half maximum (FWHM). The other peaks in these scans represent noise processes and correspond to known single- or two-photon transitions in Sr or Ca. When the transfer laser is tuned to 4607 Å, for example, $\text{Sr}(5s5p^1P_1^o)$ atoms are produced; these excited atoms collide with ground-state Ca^+ to produce $\text{Sr}^+(5p^2P_{3/2}^o)$ population by way of normal exothermic ($\sim 600 \text{ cm}^{-1}$) charge transfer.⁷ The importance of time resolved detection is now apparent in that the laser-induced charge-transfer signal decays rapidly relative to the other lines. In the laser-induced collision process, energy transfer occurs only when the laser field is present; hence, fluorescence from the target state must maximize during the time the transfer laser pulse is present and then decay at a rate which is commensurate with the lifetime of the target state,

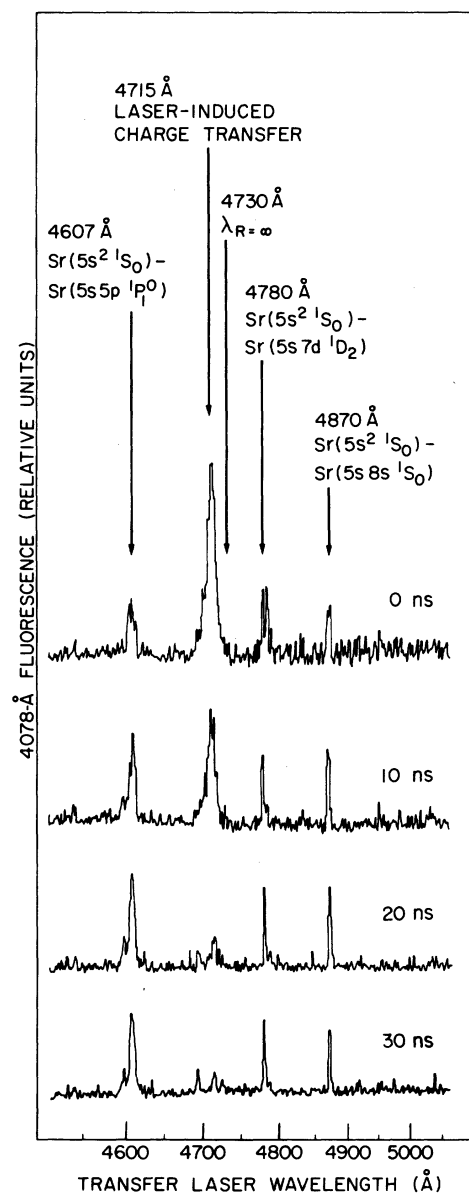


FIG. 4. Fluorescence from $\text{Sr}^+(5p^2P_{3/2}^o)$ population as a function of transfer laser wavelength and time.

which in this case is approximately 7 ns.⁸ In the other processes, energy transfer occurs as long as ions and excited neutrals are present; since these species exist for long times, so also does fluorescence.

Figure 5 presents scans associated with reaction (1b). Fluorescence at 4216 Å is plotted as a function of transfer laser wavelength for the different observation time intervals. The laser-induced charge-transfer signal is the broad curve peaking at 4795 Å and upon which other narrow lines are superimposed. The linewidth of this process is ~ 300

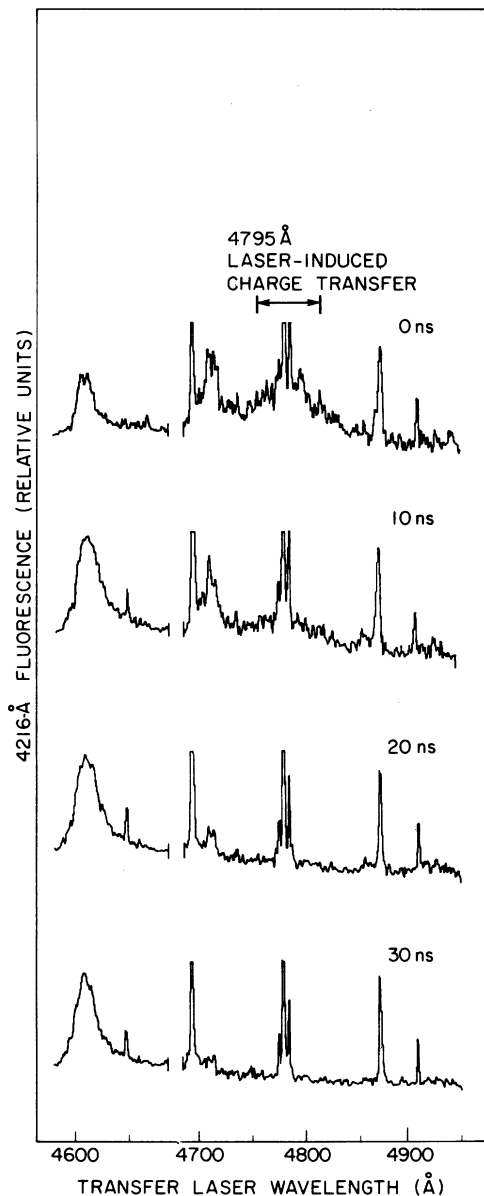


FIG. 5. Fluorescence from $\text{Sr}^+(5p^2P_{1/2}^o)$ population as a function of transfer laser wavelength and time. Signals at 4607, 4648, 4694, 4775, 4780, 4785, 4870, and 4910 Å correspond to single- and two-photon transitions in Sr and Ca, and are not labeled for purposes of clarity. The vertical sensitivity is increased by a factor of 13 at 4685 Å.

cm^{-1} , and the shape is roughly symmetrical. Note again the rapid decay of the laser-induced charge-transfer signal relative to the other lines. One exception is the line at 4715 Å, which also decays rapidly with time. The kinetics associated with this peak are probably as follows: Radiation at 4715 Å populates the $\text{Sr}^+(5p^2P_{3/2}^o)$ level via laser-

induced charge-transfer collisions; inelastic collisions then transfer this excitation to the $\text{Sr}^+(5p^3P_{1/2}^o)$ level, which fluoresces at 4216 Å. Since the $\text{Sr}^+(5p^2P_{3/2}^o)$ population decays rapidly, so must the $\text{Sr}^+(5p^3P_{1/2}^o)$ population.

Several diagnostic measurements were made to confirm the interpretation of the peaks at 4715 and 4795 Å as due to laser-induced charge-transfer collisions. These were: (1) detuning the pump laser by 10 Å from the $\text{Ca}(4s^2S_0)$ - $\text{Ca}(4s4d^1D_2)$ two-photon transition eliminated the $\text{Ca}^+(4s^2S_{1/2})$ population and caused the signals at 4715 and 4795 Å to disappear; the two-photon noise lines remained; (2) tuning the pump laser to the $\text{Sr}(5s^2S_0)$ - $\text{Sr}(5p^2S_0)$ two-photon transition produced $\text{Sr}^+(5s^2S_{1/2})$ population; no signals at 4715 or 4795 Å were observed, while two-photon lines appeared; and (3) the linewidth, shape, and position of the peaks at 4715 and 4795 Å were unaffected by changing the argon buffer-gas pressure.

The collision cross sections associated with reactions (1a) and (1b) are determined from the relation

$$\sigma = \left[\frac{N(\text{Sr}^{+*})}{N(\text{Ca}^+)} \right] \left[\frac{1}{N(\text{Sr})\bar{V}\tau} \right], \quad (2)$$

where $N(\text{Sr}^{+*})$ is the number density of excited Sr^+ created by the laser-induced charge-transfer process, $N(\text{Ca}^+)$ is the number density of ground-state Ca^+ created by the pump laser, $N(\text{Sr})$ is the number density of ground-state Sr neutrals, \bar{V} is the relative speed between Ca ions and Sr neutrals, and τ is the duration of the transfer laser pulse. $N(\text{Sr}^{+*})$ is determined from the amplitude of fluorescence as recorded by the photomultiplier and signal processing electronics in conjunction with a calibration of the transmittance of the collection optics. $N(\text{Ca}^+)$ is determined by the method of equivalent width⁹ from the absorption of a probe laser beam which is scanned through the $\text{Ca}^+(4s^2S_{1/2})$ - $\text{Ca}^+(4p^2P_{3/2}^o)$ transition. $N(\text{Sr})$ is also measured by the equivalent width method, with a white-light absorption scan. As an example of the determination of a cross section associated with reaction (1a), the following measurements were made: At a cell temperature of 850°C, the ground-state Sr density was determined to be $N(\text{Sr}) = (2.4 \pm 1.0) \times 10^{16} \text{ cm}^{-3}$. With the pump laser operating at a power density of $4 \times 10^9 \text{ W/cm}^2$, and a ground-state Ca neutral density of $N(\text{Ca}) = 6 \times 10^{15} \text{ cm}^{-3}$, the ground-state Ca^+ density was measured to be $N(\text{Ca}^+) = (4.5 \pm 2.4) \times 10^{14} \text{ cm}^{-3}$. At a transfer laser power density of $1.2 \times 10^8 \text{ W/cm}^2$, the $\text{Sr}(5p^2P_{3/2}^o)$ density was mea-

sured to be $N(\text{Sr}^{+*}) = (2.6 \pm 1.6) \times 10^{11} \text{ cm}^{-3}$. Thus, with $\bar{V} = 9.4 \times 10^4 \text{ cm/s}$, and $\tau = 5 \times 10^{-9} \text{ s}$, Eq. (2) gives $\sigma = (5.1 \pm 4.6) \times 10^{-17} \text{ cm}^2$. Further values of collision cross sections for both reactions (1a) and (1b) are plotted as a function of transfer laser power density in Fig. 6.

IV. DISCUSSION

The different experimental results obtained for the different reactions can be explained qualitatively by considering the potential energy curves of the CaSr^+ quasimolecule. Figure 7 shows the potential curves which asymptotically approach the initial and final states of reactions (1a) and (1b). These curves result from induced polarizations and van der Waals interactions, and are computed from experimental values of polarizabilities¹⁰ and oscillator strengths.^{8,11} It is apparent that the curves associated with the initial and final states of reaction (1a) are very nearly parallel. Hence, the wavelength of the photon which connects these two curves at the R where the maximum transition rate occurs is not detuned very much from the $\lambda_{R=\infty}$ wavelength (4715 Å connects the curves at $R = 8.8$ Å; $\lambda_{R=\infty} = 4730$ Å). The parallel nature of the curves also results in a narrow linewidth for the laser-induced collision process. In reaction (1b), on the other hand, it is evident from Fig. 7 that the curves associated with the initial and final states of the system are very different from one another. Thus, the photon which connects these curves at the appropriate R is detuned considerably from the $\lambda_{R=\infty}$ photon, and the linewidth is broad (4795 Å

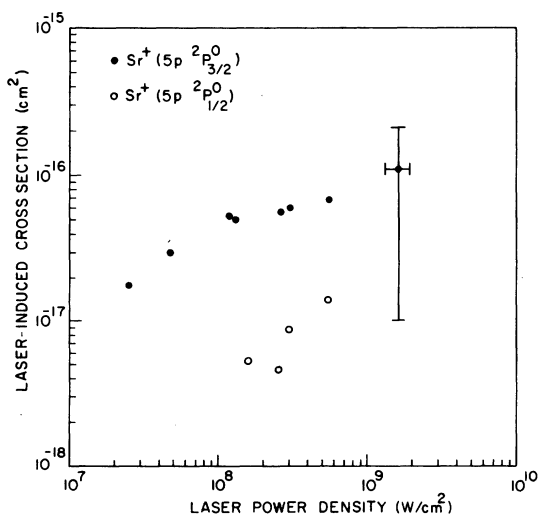


FIG. 6. Laser-induced charge-transfer cross sections as a function of transfer laser power density.

connects the curves at $R = 8.7$ Å; $\lambda_{R=\infty} = 4916$ Å). The reason for the difference in the potential curves of the two reactions is the near coincidence of the $\text{Sr}(5p \ ^2P_{1/2}^0)$ level with the resonance line of Ca.

The fact that the collision cross section associated with reaction (1a) is larger than that associated with reaction (1b) is a result of two factors. First, the detuning of a photon at 4715 Å relative to the $5s \ 5p \ ^1P_1^0$ state of the Sr atom is 500 cm^{-1} , while the detuning of a photon at 4795 Å is 850 cm^{-1} ; it is expected that the collision cross section is inversely proportional to the square of this detuning. Second, the nearly parallel quasimolecular potential-energy curves associated with the initial and final states of reaction (1a) imply a long collision interaction time, while the nonparallel curves associated with reaction (1b) imply a short interaction time.

The explanations given above regarding the distinctions between reactions (1a) and (1b) are qualitative in nature. The Landau-Zener formalism^{12,13} in conjunction with a widely used form for the charge-transfer interaction Hamiltonian¹⁴ leads to very erroneous predictions for reactions (1a) and (1b), i.e., collision cross sections which are an order of magnitude larger than those measured, and line shapes which peak farther from $\lambda_{R=\infty}$ and are much broader than those observed.

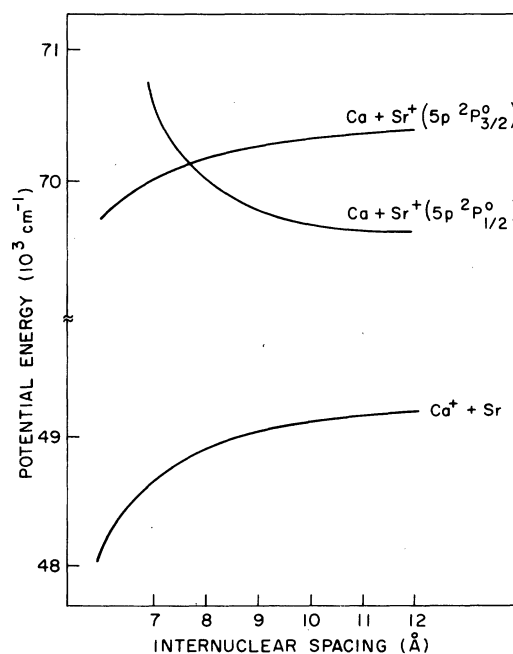


FIG. 7. Quasimolecular potentials associated with reactions (1a) and (1b).

ACKNOWLEDGMENTS

The authors gratefully acknowledge the contributions of B. Yoshizumi and G. Zdasiuk. This work

was supported by the U. S. Air Force Office of Scientific Research under Contract No. F49620-80-C-0023.

-
- ¹L. I. Gudzenko and S. I. Yakovlenko, Zh. Tekh. Fiz. **45**, 234 (1975) [Sov. Phys.—Tech. Phys. **20**, 150 (1975)].
- ²R. Z. Vitlina, A. V. Chaplik, and M. V. Entin, Zh. Eksp. Teor. Fiz. **67**, 1667 (1974) [Sov. Phys.—JETP **40**, 829 (1974)].
- ³D. A. Copeland and C. L. Tang, J. Chem. Phys. **65**, 3161 (1976); **66**, 5126 (1977).
- ⁴M. H. Nayfeh and M. G. Payne, Phys. Rev. A **17**, 1695 (1978).
- ⁵W. R. Green, M. D. Wright, J. F. Young, and S. E. Harris, Phys. Rev. Lett. **43**, 120 (1979).
- ⁶L. S. Goldberg and C. A. Moore, in *Laser Spectroscopy*, edited by R. G. Brewer and A. Mooradian (Plenum, New York, 1974).
- ⁷N. Dutta, R. Tkach, D. Frohlich, C. L. Tang, H. Mahr, and P. L. Hartman, Phys. Rev. Lett. **42**, 175 (1979).
- ⁸A. Gallagher, Phys. Rev. **157**, 24 (1967).
- ⁹A. P. Thorne, *Spectrophysics* (Chapman and Hall, London, 1974), pp. 307–311.
- ¹⁰T. M. Miller and B. Bederson, in *Advances in Atomic and Molecular Physics*, edited by D. R. Bates and B. Bederson (Academic, New York, 1977), Vol. 13, p. 32.
- ¹¹W. L. Wiese, M. W. Smith, and B. M. Miles, *Atomic Transition Probabilities: Volume II, Sodium Through Calcium* (U. S. Government Printing Office, Washington, D. C., 1969), p. 248.
- ¹²L. D. Landau, Phys. Z. Sowjetunion **2**, 46 (1932).
- ¹³C. Zener, Proc. R. Soc. London **A137**, 696 (1932).
- ¹⁴R. E. Olson, F. T. Smith, and E. Bauer, Appl. Opt. **10**, 1848 (1971).